Author Manuscript

Author Manuscript

Author Manuscript

Author Manuscript

HHS Public Access

Author manuscript

Tribol Int. Author manuscript; available in PMC 2020 October 23.

Published in final edited form as:

Tribol Int. 2019 May ; 133: 101–110. doi:10.1016/j.triboint.2019.01.014.

Predicting the polyethylene wear rate in pin-on-disc experiments in the context of prosthetic hip implants: deriving a data-driven model using machine learning methods

A. Borjali[1], **K. Monson**[1], **B. Raeymaekers**[1,*]

[1]Department of Mechanical Engineering, University of Utah, Salt Lake City, UT 84112, USA

Abstract

Pin-on-disc (PoD) experiments are widely used to quantify and rank wear of different material couples for prosthetic hip implant bearings. However, polyethylene wear results obtained from different PoD experiments are sometimes difficult to compare, which potentially leaves information inaccessible. We use machine learning methods to implement several data-driven models, and subsequently validate them by quantifying the prediction error with respect to published experimental data. A data-driven model can supplement results from PoD wear experiments, and enables predicting polyethylene wear of new PoD experiments based on its operating parameters. It also reveals the relative contribution of individual PoD operating parameters to the resulting polyethylene wear, thus informing design of experiments, and potentially reducing the need for time consuming PoD wear measurements.

Keywords

Prosthetic hip implant; polyethylene wear; pin-on-disc; machine learning

1. Introduction

A prosthetic hip implant typically comprises a femoral component that articulates with an acetabular component to replace the natural hip function and alleviate pain and disability from degenerative joint diseases such as (osteo)arthritis [1]. Metal-on-polyethylene (MoP) is the most commonly used bearing material couple in state-of-the-art prosthetic hip implants used in the United States [2], typically pairing a CoCrMo femoral head with a polyethylene acetabular liner. Many studies document the effect of polyethylene wear on the longevity of MoP prosthetic hip implants (see e.g. [3-5]). Polyethylene wear debris may cause osteolysis ("weakening of the bone") [4], which could potentially lead to implant loosening and mechanical instability [5]. Research to reduce polyethylene wear and increase longevity of MoP prosthetic hip implants involves changing the implant design and improving the

*Corresponding author: bart.raeymaekers@utah.edu.

Publisher's Disclaimer: This is a PDF file of an unedited manuscript that has been accepted for publication. As a service to our customers we are providing this early version of the manuscript. The manuscript will undergo copyediting, typesetting, and review of the resulting proof before it is published in its final citable form. Please note that during the production process errors may be discovered which could affect the content, and all legal disclaimers that apply to the journal pertain.

Author Manuscript Author Manuscript Author Manuscript Author Manuscript

mechanical properties of the polyethylene liner. For instance, highly cross-linked polyethylene (HXPE) and vitamin-E infused/blended cross-linked polyethylene (VEXPE) show significantly reduced wear compared to conventional ultra-high molecular weight polyethylene (UHMWPE) both in-vitro [6] and in-vivo [7]. On the other hand, using new materials for the femoral component, such as titanium [8], zirconia [9-11], silicon nitride [12], and tungsten [13], and manufacturing ultra-smooth ceramic bearing surfaces [14] or microtexturing the metal bearing surface [15-19] also reduces polyethylene wear.

Pin-on-disc (PoD) wear experiments are widely used as a screening method to quantify, compare, and rank wear of different implant bearing material couples as a function of operating parameters and environmental conditions. A PoD wear measurement in the context of MoP prosthetic hip implants typically consists of a polyethylene pin that is loaded against a metallic disc, while relative motion between the pin and the disc causes polyethylene wear. Many researchers have performed PoD wear experiments attempting to obtain clinically relevant polyethylene wear, using a variety of configurations. Figure 1 shows eight different PoD wear measurement configurations documented in the literature and used in the context of prosthetic hip implants. u_X and u_Y are the velocity magnitude in the x- and y-directions, respectively, and ω_Z is the angular velocity about the z-direction.

Figure 1 (a) shows a configuration in which the pin is stationary and loaded onto a disc that performs a reciprocating motion along the x-direction with velocity u_X [20-30]. Conversely, Fig. 1 (b) depicts a pin that performs a reciprocating motion along the x-direction with velocity u_X while loaded onto a stationary disc [31]. Figure 1 (c) displays a stationary pin loaded onto a disc that rotates around its center axis with angular velocity ω_Z [32-35], whereas Fig. 1 (d) depicts a pin loaded onto a stationary disc while it rotates around its center axis with angular velocity ω_Z [16,36]. The PoD wear measurement configurations of Figs. 1 (a)-(d) all create unidirectional relative motion between the pin and the disc. While these configurations allow ranking wear of different bearing material couples, the resulting polyethylene wear rate is typically one to two orders of magnitude lower than the polyethylene wear measured in retrieved prosthetic hip implants of the same material, because long polyethylene molecules align in the sliding direction [37-39]. In contrast, multidirectional motion creates cross-shear, i.e., the relative motion between pin and disc changes direction with respect to the surface of the pin, thereby avoiding polymer molecule alignment and typically resulting in polyethylene wear that is similar in magnitude to what is observed in-vivo.

Figures 1 (e)-(h) show PoD wear measurement configurations that allow creating multidirectional relative motion between the pin and the disc. Figure 1 (e) depicts a stationary pin loaded onto a disc that reciprocates with velocities u_X and u_Y in the x- and y-directions, respectively [6,37,40-62]. Furthermore, Fig. 1 (f) shows a pin reciprocating in the y-direction with velocity u_Y and loaded onto a disc reciprocating in the x-direction with velocity u_X [63]. Figure 1 (g) displays a pin that rotates around its center axis with angular velocity ω_Z and is loaded onto a disc that reciprocates in the x-direction with velocity u_X [64-67]. Finally, Fig. 1 (h) shows a pin that is loaded onto the disc and rotates around an axis parallel to the disc axis with eccentricity e and with angular velocity $\omega_{Z,2}$, while the disc rotates around its center axis with angular velocity $\omega_{Z,1}$ [15,68-75].

Author Manuscript Author Manuscript Author Manuscript Author Manuscript

PoD wear experiments typically require defining several operating parameters. For instance, different multidirectional wear paths have been documented in the literature, such as rectangular [15,40,53,57-60,68,71], elliptical [42,44,48,49,61], circular [6,43,45,47,51,52], square [56,69,70,72-75], and random [54,55]. The circular and elliptical wear paths create cross-shear on the surface of the pin throughout the entire wear path, whereas the rectangular and square wear paths create cross-shear when the pin changes direction along the wear path. Furthermore, several researchers report a strong correlation between polyethylene wear and both contact area and contact pressure between the pin and the disc (or the normal load applied to the pin) [51,55,69]. Polyethylene wear is also dependent on the surface roughness of the disc surface [26,43,76,77] and on the lubricant used during the PoD wear experiment. Although bovine serum is typically used as lubricant for PoD wear experiments in the context of prosthetic hip implants [78], the optimal composition of bovine serum remains subject to debate. Studies have reported that polyethylene wear is a function of bovine serum protein concentration [52,79], protein type [80], lipid concentration [45], dilution method [75], and anti-bacterial and fungal additives [73,81]. Another important factor reported in the literature is the radiation dose of HXPE [82]; increasing the radiation dose increases polyethylene cross-linking, which in turn increases its wear resistance. However, some reports also document decreasing fracture resistance with increasing radiation dose [83]. Radiation may also leave residual free radicals in the polyethylene that can cause oxidation over time [84]. Re-melting [85] or adding free radical scavenger agents such as vitamin-E to the HXPE [41,86,87] can reduce the risk of oxidation.

A large number of polyethylene wear datasets obtained using PoD wear experiments, conducted in the context of prosthetic hip implants, exists in the literature. These experiments are performed by different research groups, using different devices, configurations, and operating conditions. Thus, results of different PoD wear experiments are sometimes difficult to compare, which potentially leaves valuable information inaccessible. Also, several limitations exist to conducting PoD wear experiments. The viscoelastic nature of polyethylene necessitates performing PoD wear experiments at a strain rate that is identical to what occurs in-vivo [88], resulting in a kinematic cycle of 1-2 Hz to mimic the human gait cycle frequency [89]. Many million kinematic cycles are needed to obtain measurable wear of the polyethylene bearing surface, which is time consuming. In addition, manufacturing pin and disc specimens to specific standards [90-92], and performing gravimetric polyethylene wear measurements also requires trained personnel [78,93].

However, in recent years, materials researchers (among others) have used machine learning methods in combination with existing datasets, to facilitate modeling complex relationships between material constituents, structure, and the corresponding mechanical properties [94]. Such data-driven models enable comparing existing datasets and predicting new results based on the existing knowledge embedded in the model, which are otherwise difficult or time consuming to obtain using traditional experimental methods [95].

Hence, the objective of this work is to aggregate published PoD polyethylene wear datasets specifically performed in the context of prosthetic hip implants, and use machine learning methods to implement a data-driven model that allows predicting the polyethylene wear rate

Author Manuscript Author Manuscript Author Manuscript Author Manuscript

of PoD wear experiments based on its operating parameters. Such a model potentially supplements PoD wear experiments and may reveal hidden relationships between polyethylene wear and PoD operating parameters. Furthermore, the model assists researchers with design of experiments (DoE) by identifying and ranking the operating parameters that most significantly affect polyethylene wear in PoD wear experiments. This allows prioritizing operating parameters considered in future PoD wear experiments, and ultimately reducing the number of experiments one must conduct. Finally, a data-driven model based on the published literature also facilitates validating new experiments and detecting outlier results.

2. Methods

2.1 Data acquisition

We perform a literature survey to collect published polyethylene wear data from PoD wear experiments, conducted by others in the context of prosthetic hip implants. The entire dataset is available in the Supplementary Material. We search the Google Scholar and PubMed databases, using keywords including “UHMWPE”, “wear”, “hip” and “pin-on-disc/disk”. We restrict our search to these keywords because polyethylene wear is dependent on the operating conditions of the PoD wear experiments, which may differ significantly depending on the application for which they are intended; e.g. operating conditions for knee and hip PoD wear experiments could be significantly different [96]. We only consider studies that imposed multidirectional motion between a polyethylene pin and a CoCr disc, with flat-on-flat geometry to control for the effect of specimen geometry, and with bovine serum as lubricant. Furthermore, we only retain studies with clearly defined and reported operating parameters (which we refer to as input attributes) and polyethylene wear rate results (which we refer to as the target attribute), and we eliminate studies where this information is either ambiguous, such as, a random wear path, or is not fully reported (more than two attributes with missing values). All data in this work is based on gravimetric polyethylene wear measurements only, which avoids inaccuracies due to plastic deformation, creep, and fluid absorption (when a soak control specimen is used) [97]. We quantify polyethylene wear using the “wear rate [mg/MC]”, which is defined as the material loss per million cycles (MC), and prescribed in the ASTM F732 standard. Some studies report the wear factor instead, which is the wear volume per unit of normal load and sliding distance [39]. Since the wear factor implicitly assumes that wear is independent of contact area [98], which may contradict in-vitro and in-vivo polyethylene wear observations in prosthetic hip implants [39], we convert the wear factor to wear rate by multiplying it by the sliding distance, normal load, and polyethylene density. We use the polyethylene density reported in each study; in cases of missing polyethylene density, we use the UHMWPE density reported in the literature (0.93 mg/mm^3 [43]). For dynamic normal loading used in some PoD wear experiments, we report the maximum value. We average a parameter’s value if it is reported as a range in any of the studies we consider.

Because their effect on the polyethylene wear rate is well-documented in the literature, we include the following PoD wear experiment operating parameters (input attributes) in the data-driven model that describes and predicts the polyethylene wear rate (target attribute) in

Author Manuscript Author Manuscript Author Manuscript Author Manuscript

PoD wear experiments: normal load [N], contact area [mm^2], frequency [Hz], sliding distance per cycle [mm/C], wear path aspect ratio, lubricant temperature [°C], lubricant protein concentration [mg/ml], disc average surface roughness (R_a) [μm], polyethylene radiation dose [kGy], and test duration [MC].

2.2 Descriptive statistics

We quantify the linear (Pearson's) correlation coefficient between each input attribute and the target attribute, normalized by the maximum correlation coefficient computed between any of the input attributes and the target attribute, to determine the relative contribution of each input attribute to the target attribute. We also determine the minimum, maximum, average, standard deviation, and stability (S) of each input attribute to characterize the dataset. The stability S is the ratio of the number of occurrences of the most frequent value of a dataset and the total number of values in that dataset, which indicates how constant an input attribute is. An input attribute with high S is almost constant and likely does not capture the entire range of that attribute's possible values. Thus, the data-driven model may underestimate the effect of that input attribute on the target attribute.

2.3 Numerical experiment

We conduct two sets of numerical experiments. First, we apply machine learning methods to the entire polyethylene wear rate dataset and the corresponding PoD wear experiment operating parameters, to determine the method that represents the entire dataset with the highest prediction accuracy. Second, we divide the polyethylene wear rate dataset into subgroups based on the polyethylene radiation dose, because it is well-known that polyethylene radiation dose affects polyethylene wear and, thus, we expect these subgroups to have similar wear rates. The three subgroups are: (1) non-irradiated, 0 kGy radiation dose, (2) conventional with radiation dose between 20 and 55 kGy, and (3) HXPE with radiation dose in excess of 70 kGy. We then apply machine learning methods to each subgroup and compare the prediction accuracy of each method to the one obtained without subgroups.

2.4 Machine learning methods

We use three types of machine learning methods, which we briefly describe in this section, and we cite references that contain details of each method, as these are not the focus of this paper. First, we employ interpretable model-based methods, in which the relationship between input and target attributes is explicitly defined, including linear regression [99], CART [100], M5 [101], random forest [102] and gradient boosting [103]. These methods train a data-driven model on the polyethylene wear rate dataset to predict the polyethylene wear rate of PoD wear experiments based on the operating parameters (input attributes, see last paragraph of Section 2.1). We use linear regression based on the least-squares method to fit weighting factors to each operating parameter and quantify its contribution to the resulting polyethylene wear rate. This allows understanding whether the relationship between the operating parameters and the polyethylene wear rate can be captured by a single linear model. CART builds a decision tree model, where nodes represent decision points, and where each branch of the tree is a separate linear regression model, i.e., different parts of the data are modeled by distinct regression models. Thus, we use this method to investigate the effect of modeling different segments of the polyethylene wear rate dataset with various

Author Manuscript Author Manuscript Author Manuscript Author Manuscript

linear regression models, optimizing the CART tree by tuning the depth of the tree and the number of leaves per node, and pruning. M5 is similar to CART but minimizes the sum rather than the mean of the error of all linear regression models that constitute the CART decision tree. We use the random forest method to investigate whether combining multiple CART trees reduces the prediction error of the data-driven model compared to using a single CART tree. The random forest method predicts the polyethylene wear rate by averaging the predicted polyethylene wear rate of multiple CART trees. In addition to the CART parameters, we also tune the number of trees in the random forest to minimize the prediction error. Gradient boosting also allows combining several CART trees into one data-driven model. While in the random forest method each tree is added to the forest independent of the other trees, gradient boosting adds each new tree specifically to improve the performance of weak trees.

Second, we use non-interpretable model-based methods including artificial neural network (ANN) [104] and support vector machine (SVM) [105]. These methods train a model on the dataset, without explicitly defining the relationship between input and target attributes, but creating a black-box model instead. ANN relates the operating parameters to the polyethylene wear rate by means of neurons that communicate with each other in a nonlinear fashion, trained by the polyethylene wear rate dataset. We implement ANN by tuning the number of hidden layers, number of nodes per layer, and the learning rate of the neural network as commonly implemented in the machine learning literature [106]. SVM fits a hyperplane through the polyethylene wear rate dataset by minimizing the error between the predicted and actual wear rate.

Third, we implement instance-based methods such as the k-nearest neighbor (KNN) method [107], which predicts the polyethylene wear rate based on the most similar instances in the dataset. Such methods handle complicated datasets that cannot be captured by a single model. Specifically, the KNN method compares unseen data against all other instances in the dataset to find its k nearest neighbors, i.e., its k most similar data points. Then, the unseen data is assigned a value based on the weighted average value of its neighbors'. We tune the number of nearest neighbors k and the weighting function in our model.

We employ tenfold cross-validation to evaluate the prediction error of the data-driven models of the polyethylene wear rate that we implement using different machine learning methods. Cross-validation involves randomly dividing the dataset into m equal subsets (so-called folds). Then, we use m-1 subsets to train the data-driven model and we use one remaining subset to validate the model. We repeat this process m times such that we validate the model on each subset exactly once. Finally, we obtain a single prediction error for each model by averaging the results of the m iterations. It is important to note that the model validation process is always performed on the one subset that has not been used to train the data-driven model, i.e., it is validated using data not used to train the model. Thus, the advantage of cross-validation compared to other validation methods, such as e.g. the hold out method, is that every data point is in the validation dataset exactly once, and is in the training dataset m-1 times [108]. In contrast, using the hold-out method for validation requires partitioning the data in a training and validation set and, thus, the validation may be significantly different depending on how the partitioning is performed.

Author Manuscript Author Manuscript Author Manuscript Author Manuscript

Commonly used metrics to evaluate the prediction error of a data-driven model include the mean absolute error (*MAE*), root mean square error (*RMSE*), and the square of the correlation coefficient (R^2) [94]. A combination of these three metrics yields a good indication of the accuracy of the data-driven model [109]. The *MAE* is given as

$$MAE = \frac{\sum_{i=1}^{n} \mid a_i - p_i \mid}{n}, \tag{1}$$

where a_i and p_i are the actual and predicted values of the i^{th} data point, respectively, and n is the total number of data points in the dataset. *RMSE* is computed as

$$RMSE = \sqrt{\frac{\sum_{i=1}^{n} (a_i - p_i)^2}{n}}, \tag{2}$$

and, R^2 is calculated as

$$R^2 = 1 - \frac{\sum_{i=1}^{n} (a_i - p_i)^2}{\sum_{i=1}^{n} (a_i - \bar{a})^2}, \tag{3}$$

3. Results and discussion

Table 1 shows the descriptive statistics of the entire polyethylene wear rate dataset consisting of 129 data points from 29 different studies that we retain from published literature based on the criteria we define in Section 2.1, and that we use to implement the different machine learning methods of Section 2.4. The literature shows that the size of a dataset to predict material properties is typically small compared to other research fields [110]. Other studies use datasets ranging from just a few data points (14 data points [111]) to tens and hundreds of data points (82 data points [112], 121 data points [113], 157 data points [114], and 218 data points [115]).

We report minimum and maximum values in Table 1 with the same number of significant digits as in their respective publications. Note that the wear path shape reports the minimum and maximum number of occurrences, i.e., one experiment used a 10 × 20 mm rectangular wear path, whereas 39 experiments used a d =10 mm circular wear path. We exclude the input attributes “lubricant protein concentration” and “lubricant temperature” from our analysis due to a high number of missing values, i.e., they are often not reported in their respective publications. We replace the four missing average disc surface roughness R_a value with the average value of the dataset (0.05 μm), which is a common practice in the machine learning literature [116].

Figure 2 shows the normalized linear correlation coefficient (see Section 2.2) between each operating parameter (input attribute) and the polyethylene wear rate (target attribute), quantifying the relative contribution of each input attribute to the target attribute. Different published studies evaluate the relative contribution of one or two operating parameters to the polyethylene wear rate. In contrast, the results of Fig. 2 leverage all PoD polyethylene wear

Author Manuscript Author Manuscript Author Manuscript Author Manuscript

rate data published in the literature (and retained for this work) and quantify the relative contribution of all operating parameters described in this work (see Section 2.1) to the resulting polyethylene wear rate. We observe that the contact area between the pin and the disc is the most important factor that affects the polyethylene wear rate, as expected, and in agreement with clinical results. For instance, MoP prosthetic hip implants show increasing wear rate with increasing femoral head size (i.e., increasing contact area between femoral head and polyethylene liner) [39]. The polyethylene radiation dose, which indicates the level of cross-linking, is the second most important input attribute, followed by the normal load, average surface roughness R_a of the disc, wear path aspect ratio (i.e., cross-shear), test duration, and sliding distance per cycle. Ranking of the relative contribution of operating parameters to the polyethylene wear rate provides guidance to designing and conducting future PoD wear experiments. Indeed, operating parameters should be included in PoD wear experiments prioritized according to this ranking, as the effect of lower ranked operating parameters on polyethylene wear could be within the noise level of the higher ranked ones. We note that although the normalized linear correlation between the frequency and the polyethylene wear rate is almost zero, its high stability value (S = 44.9%) indicates that the dataset only spans a small range (1.8 Hz) and, thus, the effect of frequency on the polyethylene wear rate might not be evident from the aggregate dataset, because most researchers recognize that polyethylene is viscoelastic, and therefore performed the PoD wear experiments at a frequency that is similar to the human gait frequency.

Table 2 shows the prediction error (*MAE, RMSE,* and R^2) of the different machine learning methods we implement in this work, based on the entire polyethylene wear rate dataset. From Table 2 we observe that KNN yields the smallest prediction error (MAE = 1.38 mg/MC) of the polyethylene wear rate compared to all other methods, after tenfold cross-validation. Thus, the KNN model predicts the polyethylene wear rate within 1.38 mg/MC for any new PoD experiment with input attributes that fall within the range of those of the dataset used to develop the model. Furthermore, these results show that an instance-based method (KNN) outperforms both interpretable and non-interpretable model-based methods, which indicates that the relationship between the operating parameters and the polyethylene wear rate is not easily captured by one single model.

Figure 3 (a) shows the experimental polyethylene PoD wear rate (red square markers) of all published studies included in our dataset, ranked by descending wear rate, and the corresponding wear rate predicted using the cross-validated data-driven model based on the KNN method (blue circle markers). In addition, Fig. 3 (b) shows the prediction error between the KNN data-driven model and the published wear data, defined for each individual study as the absolute value of the difference between the experimental and the predicted result, divided by the experimental result (black triangle markers). From Fig. 3 (a) we observe that when the wear rate exceeds 15 mg/MC (indicated as region (a) in Fig. 3 (a)), the predicted polyethylene wear rate deviates from the corresponding experimental results by 5 to 47%. This is due to the lack of data to train the model in this region, as only eight out of 129 experiments report a polyethylene wear rate in excess of 15 mg/MC. Since KNN is an instance-based method, it requires more “instances” to train itself and lower the prediction error for polyethylene wear rate higher than 15 mg/MC.

Author Manuscript Author Manuscript Author Manuscript Author Manuscript

Furthermore, Fig. 3 (a) highlights several studies using labels (b) to (l), for which the data-driven model results in a prediction error that exceeds 4%. The high prediction error for these specific studies is because they display a unique feature that differs significantly from the rest of the dataset, which cannot be fully captured by the data-driven model. Studies (b) and (d) are performed by the same research group [69] and are the only experiments in the dataset that change the composition of the lubricant while the experiment was ongoing; specifically, the lubricant composition changes after 0.5 MC and continues with a different composition for 1 MC. Study (c) intentionally uses a significantly higher lubricant protein concentration (the maximum lubricant protein concentration in the dataset of 64.8 mg/ml) than what other wear experiments typically use (approximately 20-30 mg/ml [52]) to generate a higher polyethylene wear rate [15], which causes the data-driven model to underestimate the polyethylene wear rate for this specific study. On the other hand, study (g) uses a significantly lower lubricant protein concentration (the minimum protein concentration in the dataset of 0.69 mg/ml) than what others commonly use [56], which results in the data-driven model overestimating the polyethylene wear rate for that study. Studies (e) [40] and (k) [41] used polyethylene infused with vitamin-E antioxidant, which is not an input attribute to the data-driven model because few published studies document the PoD polyethylene wear rate of VEXPE. Thus, the model is not trained to account for these parameters. Study (f) [45] is the only study that uses a frequency (0.2 Hz) outside of the ASTM F732 standard recommended frequency range (0.5 to 2.0 Hz [78]). All the other studies employ frequencies between 1 and 2 Hz. Study (h) [57] performs heat treatment on the polyethylene after cross-linking, which we do not specifically consider in the data-driven model as an input attribute. Furthermore, the polyethylene of study (h) is the only polyethylene that is manufactured by the same research group who evaluates polyethylene wear of several commercially available cross-linked polyethylene materials. Hence, the prediction error of the data-driven model also potentially identifies manufacturing defects. Study (i) and (j) are performed by the same research group [68] who use a rectangular wear path for PoD wear experiments, with the highest (1 × 9 mm) and the second highest (2 × 8 mm) aspect ratio in the dataset, indicating one direction is dominant. A unidirectional wear path is well-known to generate a significantly lower polyethylene wear rate compared to a multidirectional wear path because of cross-shear. Since the data-driven model in this work is trained on the polyethylene wear rate dataset obtained with multidirectional relative motion between the pin and the disc, it significantly overestimates the polyethylene wear rate in these two studies. Finally, study (l) uses the smallest contact area and normal load in the dataset [47], which are well below the ASTM F732 recommended values (contact area 63.6 mm^2 and normal load corresponding to 2 to 10 MPa contact pressure [78]).

Table 2 also shows that CART is the interpretable model-based method with the lowest mean absolute error (1.95 mg/MC). Although the CART method shows a higher prediction error than the KNN method for the dataset of this work, it allows creating an interpretable model of the dataset. Figure 4 illustrates the first seven nodes of the CART model of the polyethylene wear rate dataset. Each node shows an operating parameter and reflects a decision whether that operating parameter is smaller than or equal to (≤ i.e., left branch) or larger than (>, i.e., right branch) the specified value at the node. From Fig. 4 we observe that “contact area” is the highest-level attribute in the CART decision tree for predicting the

Author Manuscript Author Manuscript Author Manuscript Author Manuscript

polyethylene wear rate, i.e., CART considers it to have the most significant effect on the polyethylene wear rate of all operating parameters considered in the model. Furthermore, we observe that for a contact area larger than 113.05 mm^2 the polyethylene wear rate is dominated by the normal load acting on the polyethylene pin, whereas for a contact area smaller than 113.05 mm^2 the polyethylene radiation dose is the deciding attribute. Similarly, one can interpret each level of the CART decision tree to obtain an understanding of how the data-driven model interprets the data and predicts results.

We also create subgroups of polyethylene wear rate data based on the polyethylene radiation dose, and implement the machine learning methods for each of these subgroups. Table 3 shows the prediction error (*MAE, RMSE,* R^2) of the different machine learning methods we implement in this study, based on each polyethylene wear rate subgroup, as defined in Section 2.3. From Table 3 we observe that clustering the data into subgroups based on the polyethylene radiation dose reduces the prediction *MAE* for the wear rate of conventional and HXPE by 10% and 64% respectively, whereas it increases the prediction *MAE* for non-irradiated polyethylene by 57%, compared to the data-driven model without clustering the data into subgroups (Table 2). The inter-quartile range of the polyethylene wear rate (the difference between the third and first quartiles of each subgroups, Q_3-Q_1) is 5.70 for non-irradiated polyethylene, whereas it is 4.64 for conventional polyethylene and 1.48 for HXPE. This indicates that the machine learning methods perform better on the subgroups with less polyethylene wear rate variability.

The primary limitation of this study is the size of the polyethylene wear rate dataset, which is inherently limited by what is available in the published literature. Ultimately, increasing the size of the dataset, as more studies are published, could increase the prediction accuracy and reduce the sensitivity of the model to noise and outlier data, such as unique features or operating parameters of specific experiments. More data would also allow considering additional input attributes in the data-driven polyethylene wear model, such as lubricant protein concentration, lubricant anti-bacterial and fungal additives, and lubricant temperature, which are parameters known to have an effect on polyethylene wear. The size of the dataset also directly affects the prediction error of the data-driven model. Furthermore, the KNN method, which results in the best prediction accuracy in our work, is limited to predict the wear rate for input attributes that fall within the range of the input attributes considered in the dataset. The model based on KNN predicts results based on the weighted average value of its k nearest neighbors, and it can only predict accurately when close neighbors exist in the dataset to that new unseen data. Considering additional input attributes, such as lubricant protein concentration, could change the structure of the dataset and, thus, the distance between the data points and nearest neighbors, which could change the KNN prediction accuracy. Another limitation of this study is that we do not distinguish between static and dynamic loading during the PoD experiments. Instead, we use the maximum load value in cases of dynamic loading.

4. Conclusion

We have aggregated a dataset of published PoD polyethylene wear rate data, performed in the context of prosthetic hip implants. Using several model-based and instance-based

Author Manuscript Author Manuscript Author Manuscript Author Manuscript

machine learning methods both with and without clustering of the data, we have implemented a data-driven model that allows predicting the PoD polyethylene wear rate based on its operating parameters.

We find that the KNN method with clustering into subgroups based on polyethylene radiation dose results in the lowest prediction error, i.e., this instance-based method outperforms interpretable and non-interpretable model-based methods, because the PoD polyethylene wear rate dataset cannot easily be captured by a single model.

The data-driven model reveals the relative contribution of PoD wear experiment operating parameters (input attributes) to the polyethylene wear rate (target attribute). This provides guidance for designing future PoD wear experiments. Operating parameters should be included in these experiments prioritized according to their relative contribution to the polyethylene wear rate, as the effect of lower ranked operating parameters on polyethylene wear could be within the noise level of the higher ranked ones.

Using cross-validation of the data-driven model we predict the polyethylene ware rate of all the experimental studies in our dataset. The data-driven model predicts results based on the subset of the dataset that is not used to train the model, at each iteration of the tenfold cross-validation process. This demonstrates that the data-driven model predicts the polyethylene wear rate for new PoD experiments with operating parameters that fall within the ranges of those of the dataset used to implement the model. This could potentially reduce the need for more experimental studies or shed light on experiment design. Furthermore, this data-driven model facilitates validating new experimental results and detecting outliers, by comparing them to results in the literature.

Supplementary Material

Refer to Web version on PubMed Central for supplementary material.

Acknowledgments

A.B. and B.R. acknowledge support from the National Institutes of Health, National Institute of Arthritis and Musculoskeletal and Skin Diseases under grant 1R03AR066826-01A1.

References

[1]. López-López JA, Humphriss RL, Beswick AD, Thom HHZ, Hunt LP, Burston A, et al. Choice of implant combinations in total hip replacement: systematic review and network meta-analysis. BMJ 2017;359:j4651. doi:10.1136/bmj.j4651. [PubMed: 29097396]

[2]. Parsons C, Batson R, Reighard S, Tanner S, Snider B, Pace TB. Clinical outcomes assessment of three similar hip arthroplasty bearing surfaces. Orthop Rev (Pavia) 2014;6:5334. doi:10.4081/or.2014.5334. [PubMed: 25002938]

[3]. Badarudeen S, Shu AC, Ong KL, Baykal D, Lau E, Malkani AL. Complications After Revision Total Hip Arthroplasty in the Medicare Population. J Arthroplasty 2017;32:1954–8. doi:10.1016/j.arth.2017.01.037. [PubMed: 28236550]

[4]. Sadoghi P, Liebensteiner M, Agreiter M, Leithner A, Böhler N, Labek G. Revision Surgery After Total Joint Arthroplasty: A Complication-Based Analysis Using Worldwide Arthroplasty Registers. J Arthroplasty 2013;28:1329–32. [PubMed: 23602418]

Author Manuscript Author Manuscript Author Manuscript Author Manuscript

[5]. Ulrich SD, Seyler TM, Bennett D, Delanois RE, Saleh KJ, Thongtrangan I, et al. Total hip arthroplasties: What are the reasons for revision? Int Orthop 2008;32:597–604. doi:10.1007/s00264-007-0364-3. [PubMed: 17443324]

[6]. Baykal D, Siskey RS, Haider H, Saikko V, Ahlroos T, Kurtz SM. Advances in tribological testing of artificial joint biomaterials using multidirectional pin-on-disk testers. J Mech Behav Biomed Mater 2014;31: 117–34. doi:10.1016/j.jmbbm.2013.05.020. [PubMed: 23831149]

[7]. Kurtz SM, Gawel HA, Patel JD. History and Systematic Review of Wear and Osteolysis Outcomes for First-generation Highly Crosslinked Polyethylene. Clin Orthop Relat Res 2011;469:2262–77. doi:10.1007/s11999-011-1872-4. [PubMed: 21431461]

[8]. Ruggiero A, D'Amato R, Gómez E, Merola M. Experimental comparison on tribological pairs UHMWPE/TIAL6V4 alloy, UHMWPE/AISI316L austenitic stainless and UHMWPE/AL2O3 ceramic, under dry and lubricated conditions. Tribol Int 2016;96:349–60. doi:10.1016/J.TRIBOINT.2015.12.041.

[9]. Lachiewicz PF, Kleeman LT, Seyler T. Bearing Surfaces for Total Hip Arthroplasty. J Am Acad Orthop Surg 2018;26:45–57. doi:10.5435/JAAOS-D-15-00754. [PubMed: 29303922]

[10]. Yang Y, Ong JL, Tian J. Deposition of highly adhesive ZrO2 coating on Ti and CoCrMo implant materials using plasma spraying. Biomaterials 2003;24:619–27. doi:10.1016/S0142-9612(02)00376-9. [PubMed: 12437956]

[11]. Sonohata M, Kitajima M, Kawano S, Mawatari M. Wear of XLPE Liner against Zirconium Heads in Cementless Total Hip Arthroplasty for Patients under 40 Years of Age. HIP Int 2017;27:532–6. doi:10.5301/hipint.5000513. [PubMed: 28574118]

[12]. Olofsson J, Grehk TM, Berlind T, Persson C, Jacobson S, Engqvist H. Evaluation of silicon nitride as a wear resistant and resorbable alternative for total hip joint replacement. Biomatter 2012;2:94–102. doi:10.4161/biom.20710. [PubMed: 23507807]

[13]. Aherwar A, Patnaik A, Bahraminasab M, Singh A. Preliminary evaluations on development of new materials for hip joint femoral head. Proc Inst Mech Eng Part L J Mater Des Appl 2017:146442071771449. doi:10.1177/1464420717714495.

[14]. Affatato S, Ruggiero A, Merola M. Advanced biomaterials in hip joint arthroplasty. A review on polymer and ceramics composites as alternative bearings. Compos Part B Eng 2015;83:276–83. doi:10.1016/J.COMPOSITESB.2015.07.019.

[15]. Langhorn J, Borjali A, Hippensteel E, Nelson W, Raeymaekers B. Microtextured CoCrMo alloy for use in metal-on-polyethylene prosthetic joint bearings: Multi-directional wear and corrosion measurements. Tribol Int 2018;124:178–83. doi:10.1016/J.TRIBOINT.2018.04.007. [PubMed: 30778273]

[16]. Borjali A, Langhorn J, Monson K, Raeymaekers B. Using a patterned microtexture to reduce polyethylene wear in metal-on-polyethylene prosthetic bearing couples. Wear 2017;392–393:77–83. doi:10.1016/J.WEAR.2017.09.014.

[17]. Qiu M, Chyr A, Sanders AP, Raeymaekers B. Designing prosthetic knee joints with bio-inspired bearing surfaces. Tribol Int 2014;77:106–10. [PubMed: 25049441]

[18]. Chyr A, Qiu M, Speltz JW, Jacobsen RL, Sanders AP, Raeymaekers B. A patterned microtexture to reduce friction and increase longevity of prosthetic hip joints. Wear 2014;315:51–7. [PubMed: 25013240]

[19]. Borjali A, Monson K, Raeymaekers B. Friction between a polyethylene pin and a microtextured CoCrMo disc, and its correlation to polyethylene wear, as a function of sliding velocity and contact pressure, in the context of metal-on-polyethylene prosthetic hip implants. Tribol Int 2018;127:568–74. doi:10.1016/J.TRIBOINT.2018.07.005. [PubMed: 30778274]

[20]. Brown KJ, Atkinson JR, Dowson D, Wright V. The wear of ultrahigh molecular weight polyethylene and a preliminary study of its relation to the in vivo behaviour of replacement hip joints. Wear 1976;40:255–64. doi:10.1016/0043-1648(76)90102-2.

[21]. McKellop H, Clarke IC, Markolf KL, Amstutz HC. Wear characteristics of UHMW polyethylene: A method for accurately measuring extremely low wear rates. J Biomed Mater Res 1978;12:895–927. doi:10.1002/jbm.820120611. [PubMed: 739020]

Author Manuscript Author Manuscript Author Manuscript Author Manuscript

[22]. Barbour PS, Stone M, Fisher J A study of the wear resistance of three types of clinically applied UHMWPE for total replacement hip prostheses. Biomaterials 1999;20:2101–6. doi:10.1016/S0142-9612(99)00096-4. [PubMed: 10555077]

[23]. Seedhom BB, Dowson D, Wright V. Wear of solid phase formed high density polyethylene in relation to the life of artificial hips and knees. Wear 1973;24:35–51. doi:10.1016/0043-1648(73)90201-9.

[24]. Galante JO, Rostoker W. Wear in Total Hip Prostheses: An Experimental Evaluation of Candidate Materials. Acta Orthop Scand 1972;43:1–46. doi:10.3109/ort.1972.43.suppl-145.01.

[25]. Deng M, Shalaby SW. Properties of self-reinforced ultra-high-molecular-weight polyethylene composites. Biomaterials 1997;18:645–55. doi:10.1016/S0142-9612(96)00194-9. [PubMed: 9151996]

[26]. Cooper JR, Dowson D, Fisher J. The effect of transfer film and surface roughness on the ear of lubricated ultra-high molecular weight polyethylene. Clin Mater 1993;14:295–302. doi:10.1016/0267-6605(93)90016-Z.

[27]. Tetreault DM, Kennedy FE. Friction and wear behavior of ultrahigh molecular weight polyethylene on Co-Cr and titanium alloys in dry and lubricated environments. Wear 1989;133:295–307. doi:10.1016/0043-1648(89)90043-4.

[28]. Dowson D, Harding RT. The wear characteristics of ultrahigh molecular weight polyethylene against a high density alumina ceramic under wet (distilled water) and dry conditions. Wear 1982;75:313–31. doi:10.1016/0043-1648(82)90156-9.

[29]. Sawyer WG, Freudenberg KD, Bhimaraj P, Schadler LS. A study on the friction and wear behavior of PTFE filled with alumina nanoparticles. Wear 2003;254:573–80. doi:10.1016/S0043-1648(03)00252-7.

[30]. Wang A, Polineni V, Essner A, Sokol M, Sun D, Stark C, et al. The Significance of Nonlinear Motion in the Wear Screening of Orthopaedic Implant Materials BT - The Significance of Nonlinear Motion in the Wear Screening of Orthopaedic Implant Materials 1997.

[31]. Burris DL, Sawyer WG. Tribological behavior of PEEK components with compositionally graded PEEK/PTFE surfaces. Wear 2007;262:220–4. doi:10.1016/J.WEAR.2006.03.045.

[32]. Kovalchenko A, Ajayi O, Erdemir A, Fenske G, Etsion I. The effect of laser surface texturing on transitions in lubrication regimes during unidirectional sliding contact. Tribol Int 2005;38:219–25. doi:10.1016/J.TRIBOINT.2004.08.004.

[33]. Xiong D, Ge S. Friction and wear properties of UHMWPE/Al2O3 ceramic under different lubricating conditions. Wear 2001;250:242–5. doi:10.1016/S0043-1648(01)00647-0.

[34]. Klapperich C, Komvopoulos K, Pruitt L. Tribological Properties and Microstructure Evolution of Ultra-High Molecular Weight Polyethylene. J Tribol 1999;121:394. doi: 10.1115/1.2833952.

[35]. Dong H, Shi W, Bell T. Potential of improving tribological performance of UHMWPE by engineering the Ti6Al4V counterfaces. Wear 1999;225–229:146–53. doi:10.1016/S0043-1648(98)00356-1.

[36]. Kumar P, Oka M, Ikeuchi K, Shimizu K, Yamamuro T, Okumura H, et al. Low wear rate of UHMWPE against zirconia ceramic (Y-PSZ) in comparison to alumina ceramic and SUS 316L alloy. J Biomed Mater Res 1991;25:813–28. doi:10.1002/jbm.820250703. [PubMed: 1918102]

[37]. Saikko V A multidirectional motion pin-on-disk wear test method for prosthetic joint materials. J Biomed Mater Res 1998;41:58–64. [PubMed: 9641624]

[38]. Kurtz SM. UHMWPE biomaterials handbook : ultra high molecular weight polyethylene in total joint replacement and medical devices. Elsevier/Academic Press; 2009.

[39]. Haider H, Baykal D. Wear Assessment of UHMWPE with Pin-on-Disc Testing UHMWPE Biomater. Handb, Elsevier; 2016, p. 553–78. doi:10.1016/B978-0-323-35401-1.00030-2.

[40]. Doshi BN, Ghali B, Godleski-Beckos C, Lozynsky AJ, Oral E, Muratoglu OK. High Pressure Crystallization of Vitamin E-containing Radiation Cross-linked UHMWPE. Macromol Mater Eng 2015;300:458–65. doi:10.1002/mame.201400294.

[41]. Oral E, Neils A, Muratoglu OK. High vitamin E content, impact resistant UHMWPE blend without loss of wear resistance. J Biomed Mater Res Part B Appl Biomater 2015;103:790–7. doi:10.1002/jbm.b.33256.

Author Manuscript Author Manuscript Author Manuscript Author Manuscript

[42]. Nakanishi Y, Nakashima Y, Fujiwara Y, Komohara Y, Takeya M, Miura H, et al. Influence of surface profile of Co-28Cr-6Mo alloy on wear behaviour of ultra-high molecular weight polyethylene used in artificial joint. Tribol Int 2018;118:538–46. doi:10.1016/j.triboint.2017.06.030.

[43]. Saikko V, Calonius O, Keränen J. Effect of counterface roughness on the wear of conventional and crosslinked ultrahigh molecular weight polyethylene studied with a multi-directional motion pin-on-disk device. J Biomed Mater Res 2001;57:506–12. [PubMed: 11553880]

[44]. Saikko V, Calonius O, Keränen J. Effect of slide track shape on the wear of ultra-high molecular weight polyethylene in a pin-on-disk wear simulation of total hip prosthesis. J Biomed Mater Res Part B Appl Biomater 2004;69B:141–8. doi:10.1002/jbm.b.20043.

[45]. Sawae Y, Yamamoto A, Murakami T. Influence of protein and lipid concentration of the test lubricant on the wear of ultra high molecular weight polyethylene. Tribol Int 2008;41:648–56.

[46]. Harsha AP, Joyce TJ. Comparative wear tests of ultra-high molecular weight polyethylene and cross-linked polyethylene. Proc. Inst. Mech. Eng. Part H J. Eng. Med, vol. 227, 2013, p. 600–8. doi:10.1177/0954411913479528.

[47]. Hua ZK, Zhang HH, Fan YW, Jin ZM. Development of a BiotriboPOD testing methodology for the wear evaluation of orthopaedic biomaterials. Rsc Adv 2014;4:19987–91. doi:10.1039/C4RA01743A.

[48]. Kurtz SM, MacDonald DW, Kocagöz S, Tohfafarosh M, Baykal D. Can Pin-on-Disk Testing Be Used to Assess the Wear Performance of Retrieved UHMWPE Components for Total Joint Arthroplasty? Biomed Res Int 2014;2014:581812. doi :10.1155/2014/581812. [PubMed: 25295264]

[49]. Hunt B, Joyce T. A Tribological Assessment of Ultra High Molecular Weight Polyethylene Types GUR 1020 and GUR 1050 for Orthopedic Applications. Lubricants 2016;4:25. doi:10.3390/lubricants4030025.

[50]. Bragdon CR, O'Connor DO, Lowenstein JD, Jasty M, Biggs SA, Harris WH. A new pin-on-disk wear testing method for simulating wear of polyethylene on cobalt-chrome alloy in total hip arthroplasty. J Arthroplasty 2001;16:658–65. doi:10.1054/arth.2001.23718. [PubMed: 11503127]

[51]. Saikko V. Effect of Contact Area on the Wear and Friction of UHMWPE in Circular Translation Pin-on-Disk Tests. J Tribol 2017;139:061606. doi:10.1115/1.4036448.

[52]. Saikko V. Effect of Lubricant Protein Concentration on the Wear of Ultra-High Molecular Weight Polyethylene Sliding Against a CoCr Counterface. J Tribol 2003;125:638. doi:10.1115/1.1537751.

[53]. Gul RM, McGarry FJ, Bragdon CR, Muratoglu OK, Harris WH. Effect of consolidation on adhesive and abrasive wear of ultra high molecular weight polyethylene. Biomaterials 2003;24:3193–9. doi:10.1016/S0142-9612(03)00165-0. [PubMed: 12763446]

[54]. Saikko V, Kostamo J. RandomPOD-A new method and device for advanced wear simulation of orthopaedic biomaterials. J Biomech 2011;44:810–4. doi:10.1016/j.jbiomech.2010.12.024. [PubMed: 21288527]

[55]. Saikko V. Effect of contact area on the wear of ultrahigh molecular weight polyethylene in noncyclic pin-on-disk tests. Tribol Int 2017;114:84–7. doi:10.1016/j.triboint.2017.04.020.

[56]. Yao JQ, Blanchet TA, Murphy DJ, Laurent MP. Effect of fluid absorption on the wear resistance of UHMWPE orthopedic bearing surfaces. Wear 2003;255:1113–20. doi:10.1016/S0043-1648(03)00167-4.

[57]. Muratoglu OK, Merrill EW, Bragdon CR, O'Connor D, Hoeffel D, Burroughs B, et al. Effect of radiation, heat, and aging on in vitro wear resistance of polyethylene. Clin Orthop Relat Res 2003;417:253–62. doi:10.1097/01.blo.0000093004.90435.d1.

[58]. Greenbaum ES, Burroughs BB, Harris WH, Muratoglu OK. Effect of lipid absorption on wear and compressive properties of unirradiated and highly crosslinked UHMWPE: An in vitro experimental model. Biomaterials 2004;25:4479–84. doi:10.1016/j.biomaterials.2003.11.049. [PubMed: 15046938]

[59]. Oral E, Wannomae KK, Hawkins N, Harris WH, Muratoglu OK. α-Tocopherol-doped irradiated UHMWPE for high fatigue resistance and low wear. Biomaterials 2004;25:5515–22. doi:10.1016/j.biomaterials.2003.12.048. [PubMed: 15142733]

Author Manuscript Author Manuscript Author Manuscript Author Manuscript

[60]. Laraia K, Leone N, MacDolanald R, Blanchet TA. Effect of water and serum absorption on wear of unirradiated and crosslinked UHMWPE orthopedic bearing materials. Tribol Trans 2006;49:338–46. doi:10.1080/05698190600678663.

[61]. Kilgour A, Elfick A. Influence of crosslinked polyethylene structure on wear of joint replacements. Tribol Int 2009;42:1582–94. doi:10.1016/j.triboint.2008.11.011.

[62]. Oral E, Ghali BW, Rowell SL, Micheli BR, Lozynsky AJ, Muratoglu OK. A surface crosslinked UHMWPE stabilized by vitamin E with low wear and high fatigue strength. Biomaterials 2010;31:7051–60. doi:10.1016/j.biomaterials.2010.05.041. [PubMed: 20579730]

[63]. Zhu X, Lauwerens W, Cosemans P, Van Stappen M, Celis J., Stals L., et al. Different tribological behavior of MoS2 coatings under fretting and pin-on-disk conditions. Surf Coatings Technol 2003;163–164:422–8. doi:10.1016/S0257-8972(02)00638-2.

[64]. Schwartz CJ, Bahadur S. Development and testing of a novel joint wear simulator and investigation of the viability of an elastomeric polyurethane for total-joint arthroplasty devices. Wear 2007;262:331–9. doi:10.1016/J.WEAR.2006.05.018.

[65]. Kang L, Galvin AL, Brown TD, Jin Z, Fisher J. Quantification of the effect of cross-shear on the wear of conventional and highly cross-linked UHMWPE. J Biomech 2008;41:340–6. doi:10.1016/J.JBIOMECH.2007.09.005. [PubMed: 17936763]

[66]. Vassiliou K, Unsworth A. Is the wear factor in total joint replacements dependent on the nominal contact stress in ultra-high molecular weight polyethylene contacts? Proc Inst Mech Eng Part H J Eng Med 2004;218:101–7. doi:10.1243/095441104322983997.

[67]. Dressier MR, Strickland MA, Taylor M, Render TD, Ernsberger CN. Predicting wear of UHMWPE: Decreasing wear rate following a change in direction. Wear 2011;271:2879–83. doi:10.1016/J.WEAR.2011.06.006.

[68]. Turell M, Wang A, Bellare A. Quantification of the effect of cross-path motion on the wear rate of ultra-high molecular weight polyethylene. Wear 2003;255:1034–9. doi:10.1016/S0043-1648(03)00357-0.

[69]. Mazzucco D, Spector M. Effects of contact area and stress on the volumetric wear of ultrahigh molecular weight polyethylene. Wear 2003;254:514–22. doi:10.1016/S0043-1648(03)00135-2.

[70]. Hill MR, Catledge SA, Konovalov V, Clem WC, Chowdhury SA, Etheridge BS, et al. Preliminary tribological evaluation of nanostructured diamond coatings against ultra-high molecular weight polyethylene 2008:140–8. doi:10.1002/jbm.b.30926.

[71]. Korduba LA, Wang A. The effect of cross-shear on the wear of virgin and highly-crosslinked polyethylene. Wear 2011;271:1220–3. doi:10.1016/j.wear.2011.01.039.

[72]. Bistolfi A, Bellare A. The relative effects of radiation crosslinking and type of counterface on the wear resistance of ultrahigh-molecular-weight polyethylene. Acta Biomater 2011;7:3398–403. doi:10.1016/j.actbio.2011.05.018. [PubMed: 21640855]

[73]. Wimmer MA, Sah R, Laurent MP, Virdi AS. The effect of bacterial contamination on friction and wear in metal/polyethylene bearings for total joint repair-A case report. Wear 2013;301:264–70. doi:10.1016/j.wear.2012.11.022.

[74]. Escudeiro A, Wimmer MA, Polcar T, Cavaleiro A. Tribological behavior of uncoated and DLC-coated CoCr and Ti-alloys in contact with UHMWPE and PEEK counterbodies. Tribol Int 2015;89:97–104. doi:10.1016/j.triboint.2015.02.002.

[75]. Guenther LE, Turgeon TR, Bohm ER, Brandt J-MM. The biochemical characteristics of wear testing lubricants affect polyethylene wear in orthopaedic pin-on-disc testing. Proc Inst Mech Eng Part H J Eng Med 2015;229:77–90. doi:10.1177/0954411914567930.

[76]. Lancaster JG, Dowson D, Isaac GH, Fisher J. The wear of ultra-high molecular weight polyethylene sliding on metallic and ceramic counterfaces representative of current femoral surfaces in joint replacement. Proc Inst Mech Eng Part H J Eng Med 1997;211: 17–24. doi:10.1243/0954411971534647.

[77]. Saikko V. Wear of polyethylene acetabular cups against zirconia femoral heads studied with a hip joint simulator. Wear 1994;176:207–12. doi:10.1016/0043-1648(94)90148-1.

[78]. ASTM F732 - 00(2011) Standard Test Method for Wear Testing of Polymeric Materials Used in Total Joint Prostheses n.d. https://www.astm.org/Standards/F732.htm (accessed July 7, 2017).

Author Manuscript Author Manuscript Author Manuscript Author Manuscript

[79]. Wang A, Essner A, Polineni V., Stark C, Dumbleton J. Lubrication and wear of ultra-high molecular weight polyethylene in total joint replacements. Tribol Int 1998;31:17–33. doi:10.1016/S0301-679X(98)00005-X.

[80]. Wang A, Essner A, Schmidig G. The effects of lubricant composition on in vitro wear testing of polymeric acetabular components. J Biomed Mater Res B Appl Biomater 2004;68:45–52. doi:10.1002/jbm.b.10077. [PubMed: 14689495]

[81]. Saikko V. Effect of Lubrication Conditions on the Wear of UHMWPE with Noncyclic Motion and Load. Tribol Trans 2018;61:1141–50. doi:10.1080/10402004.2018.1506071.

[82]. Oral E, Muratoglu OK. Radiation cross-linking in ultra-high molecular weight polyethylene for orthopaedic applications. Nucl Instruments Methods Phys Res Sect B Beam Interact with Mater Atoms 2007;265:18–22. doi:10.1016/j.nimb.2007.08.022.

[83]. Furmanski J, Anderson M, Bal S, Greenwald AS, Halley D, Penenberg B, et al. Clinical fracture of cross-linked UHMWPE acetabular liners. Biomaterials 2009;30:5572–82. doi:10.1016/J.BIOMATERIALS.2009.07.013. [PubMed: 19643471]

[84]. Brach Del Prever E, Crova M, Costa L, Dallera A, Camino G, Gallinaro P. Unacceptable biodegradation of polyethylene in vivo. Biomaterials 1996;17:873–8. doi:10.1016/0142-9612(96)83282-0. [PubMed: 8718932]

[85]. Muratoglu OK, Bragdon CR, O'Connor DO, Jasty M, Harris WH. A novel method of cross-linking ultra-high-molecular-weight polyethylene to improve wear, reduce oxidation, and retain mechanical properties: Recipient of the 1999 HAP Paul award. J Arthroplasty 2001;16:149–60. doi:10.1054/arth.2001.20540. [PubMed: 11222887]

[86]. Shen J, Gao G, Liu X, Fu J. Natural Polyphenols Enhance Stability of Crosslinked UHMWPE for Joint Implants. Clin Orthop Relat Res 2015;473:760–6. doi:10.1007/s11999-014-3850-0. [PubMed: 25106800]

[87]. Bracco P, Oral E. Vitamin E-stabilized UHMWPE for Total Joint Implants: A Review. Clin Orthop Relat Res 2011 ;469:2286–93. doi:10.1007/s11999-010-1717-6. [PubMed: 21132413]

[88]. Popelar CF, Popelar CH, Kenner VH. Viscoelastic material characterization and modeling for polyethylene. Polym Eng Sci 1990;30:577–86. doi:10.1002/pen.760301004.

[89]. Murray MP, Drought a. B, Kory RC. Walking Patterns of Normal Men. J Bone Jt Surg 1964;46:335–60.

[90]. ASTM F648 - 14 Standard Specification for Ultra-High-Molecular-Weight Polyethylene Powder and Fabricated Form for Surgical Implants n.d. https://www.astm.org/Standards/F648.htm (accessed July 10, 2017).

[91]. ASTM F2695 - 12 Standard Specification for Ultra-High Molecular Weight Polyethylene Powder Blended With Alpha-Tocopherol (Vitamin E) and Fabricated Forms for Surgical Implant Applications n.d. https://www.astm.org/Standards/F2695.htm (accessed July 10, 2017).

[92]. ASTM F1537 - 11 Standard Specification for Wrought Cobalt-28Chromium-6Molybdenum Alloys for Surgical Implants (UNS R31537, UNS R31538, and UNS R31539) n.d. https://www.astm.org/Standards/F1537.htm (accessed December 29, 2017).

[93]. ASTM F2025-06(2018), Standard Practice for Gravimetric Measurement of Polymeric Components for Wear Assessment, ASTM International, West Conshohocken, PA, 2018, n.d. https://www.astm.org/Standards/F2025.htm (accessed July 9, 2018).

[94]. Han J, Kamber M, Pei J. Data mining : concepts and techniques. Elsevier Science; 2012.

[95]. Ramprasad R, Batra R, Pilania G, Mannodi-Kanakkithodi A, Kim C. Machine learning in materials informatics: recent applications and prospects. Npj Comput Mater 2017;3. doi:10.1038/s41524-017-0056-5.

[96]. Schmalzried T, Callaghan J. Current Concepts Review - Wear in Total Hip and Knee Replacements. JBJS 1999;81.

[97]. Blunt L, Bills P, Jiang X, Hardaker C, Chakrabarty G. The role of tribology and metrology in the latest development of bio-materials. Wear 2009;266:424–31. doi:10.1016/j.wear.2008.04.015.

[98]. Zmitrowicz A. Wear patterns and laws of wear - A review. J Theor Appl Mech 2006;44:219–53.

[99]. Kilic S. Linear regression analysis. J Mood Disord 2013;3:90. doi:10.5455/jmood.20130624120840.

Author Manuscript Author Manuscript Author Manuscript Author Manuscript

[100]. Rokach L, Maimon O. Data Mining with Decision Trees: Theroy and Applications. River Edge, NJ, USA: World Scientific Publishing Co., Inc.; 2008.

[101]. Loh W-Y. Classification and regression trees. Wiley Interdiscip Rev Data Min Knowl Discov 2011;1:14–23. doi:10.1002/widm.8.

[102]. Liaw A, Wiener M. Classification and Regression by randomForest. R News 2002;2:18–22. doi:10.1023/A:1010933404324.

[103]. Sutton CD. Classification and Regression Trees, Bagging, and Boosting. Handb Stat 2004;24:303–29. doi:10.1016/S0169-7161(04)24011-1.

[104]. Dreiseitl S, Ohno-Machado L. Logistic regression and artificial neural network classification models: a methodology review. J Biomed Inform 2002;35:352–9. doi:10.1016/S1532-0464(03)00034-0. [PubMed: 12968784]

[105]. Smola AJ, Schölkopf B. A tutorial on support vector regression. Stat Comput 2004;14:199–222. doi:10.1023/B:STC0.0000035301.49549.88.

[106]. Morid MA, Fiszman M, Raja K, Jonnalagadda SR, Del Fiol G. Classification of clinically useful sentences in clinical evidence resources. J Biomed Inform 2016;60:14–22. doi:10.1016/J.JBI.2016.01.003. [PubMed: 26774763]

[107]. Hastie T, Tibshirani R. Discriminant adaptive nearest neighbor classification. IEEE Trans Pattern Anal Mach Intell 1996;18:607–16. doi:10.1109/34.506411.

[108]. Liu Y, Zhao T, Ju W, Shi S, Shi S, Shi S. Materials discovery and design using machine learning. J Mater 2017;3:159–77. doi:10.1016/j.jmat.2017.08.002.

[109]. Willmott CJ, Ackleson SG, Davis RE, Feddema JJ, Klink KM, Legates DR, et al. Statistics for the Evaluation and Comparison of Models. J Geophys Res 1985;90:8995–9005.

[110]. Zhang Y, Ling C. A strategy to apply machine learning to small datasets in materials science. Npj Comput Mater 2018;4:25. doi:10.1038/s41524-018-0081-z.

[111]. Rao HS, Mukherjee A. Artificial neural networks for predicting the macromechanical behaviour of ceramic-matrix composites. Comput Mater Sci 1996;5:307–22. doi:10.1016/0927-0256(95)00002-X.

[112]. Kim C, Pilania G, Ramprasad R. From Organized High-Throughput Data to Phenomenological Theory using Machine Learning: The Example of Dielectric Breakdown. Chem Mater 2016;28:1304–11. doi:10.1021/acs.chemmater.5b04109.

[113]. Evans JD, Coudert FX. Predicting the Mechanical Properties of Zeolite Frameworks by Machine Learning. Chem Mater 2017;29:7833–9. doi:10.1021/acs.chemmater.7b02532.

[114]. Chonghe L, Yihao T, Yingzhi Z, Chunmei W, Ping W. Prediction of lattice constant in perovskites of GdFe03structure. J Phys Chem Solids 2003;64:2147–56. doi:10.1016/S0022-3697(03)00209-9.

[115]. Wu H, Lorenson A, Anderson B, Witteman L, Wu H, Meredig B, et al. Robust FCC solute diffusion predictions from ab-initio machine learning methods. Comput Mater Sci 2017;134:160–5. doi:10.1016/j.commatsci.2017.03.052.

[116]. Batista GEAPA, Monard MC. An analysis of four missing data treatment methods for supervised learning. Appl Artif Intell 2003;17:519–33. doi:10.1080/713827181.

Author Manuscript Author Manuscript Author Manuscript Author Manuscript

Highlights

- A data-driven model predicts the PoD polyethylene wear rate
- A data-driven model reveals the relative contribution of PoD wear experiment operating parameters to the polyethylene wear rate
- A data-driven model reduces the need for additional experimental studies

Author Manuscript Author Manuscript Author Manuscript Author Manuscript

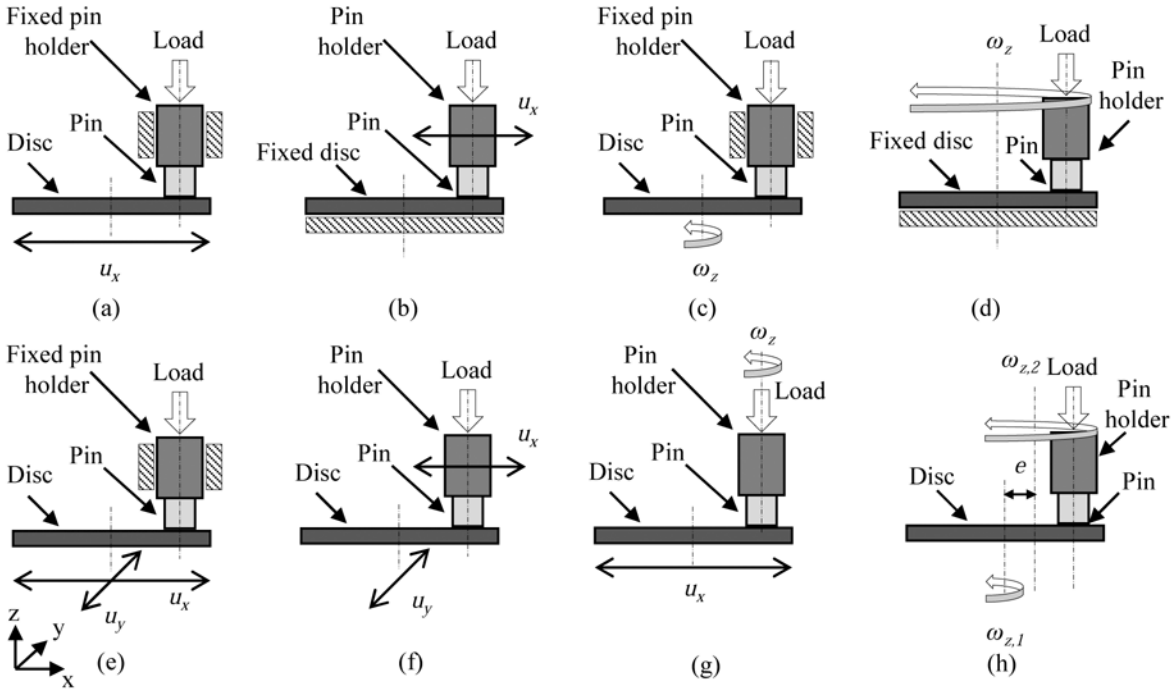

Figure 1.

Schematic of eight different PoD wear measurement configurations used in the context of prosthetic hip implants, showing the relative motion between the pin and the disc. u_x and u_y are the velocity magnitude in the *x*- and *y*-directions, and ω_z is angular velocity about the *z*-direction.

Author Manuscript Author Manuscript Author Manuscript Author Manuscript

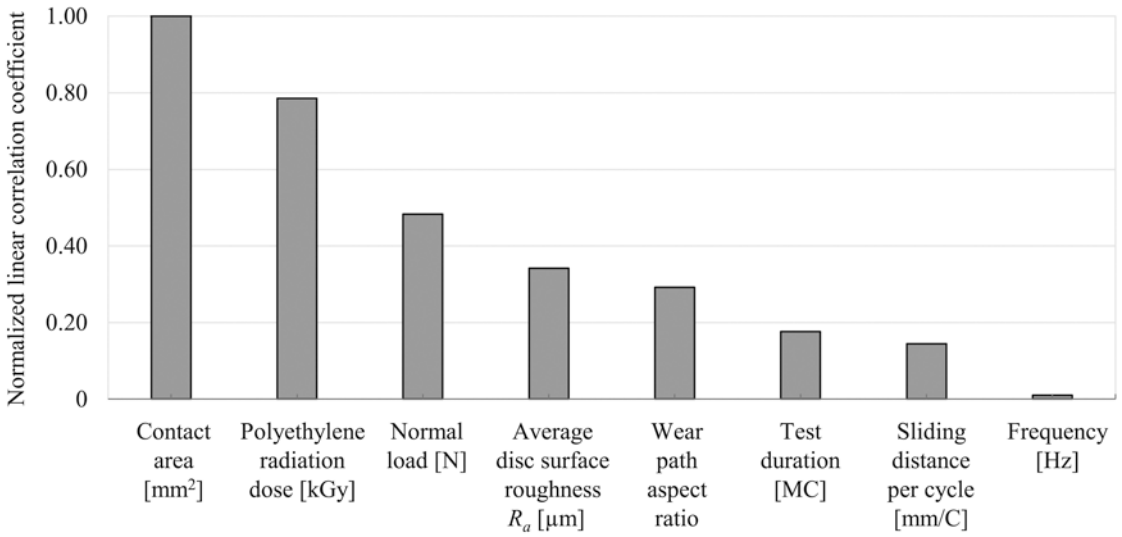

Figure 2.

Normalized linear correlation coefficient of each input attribute with the polyethylene wear rate (target attribute)

Author Manuscript Author Manuscript Author Manuscript Author Manuscript

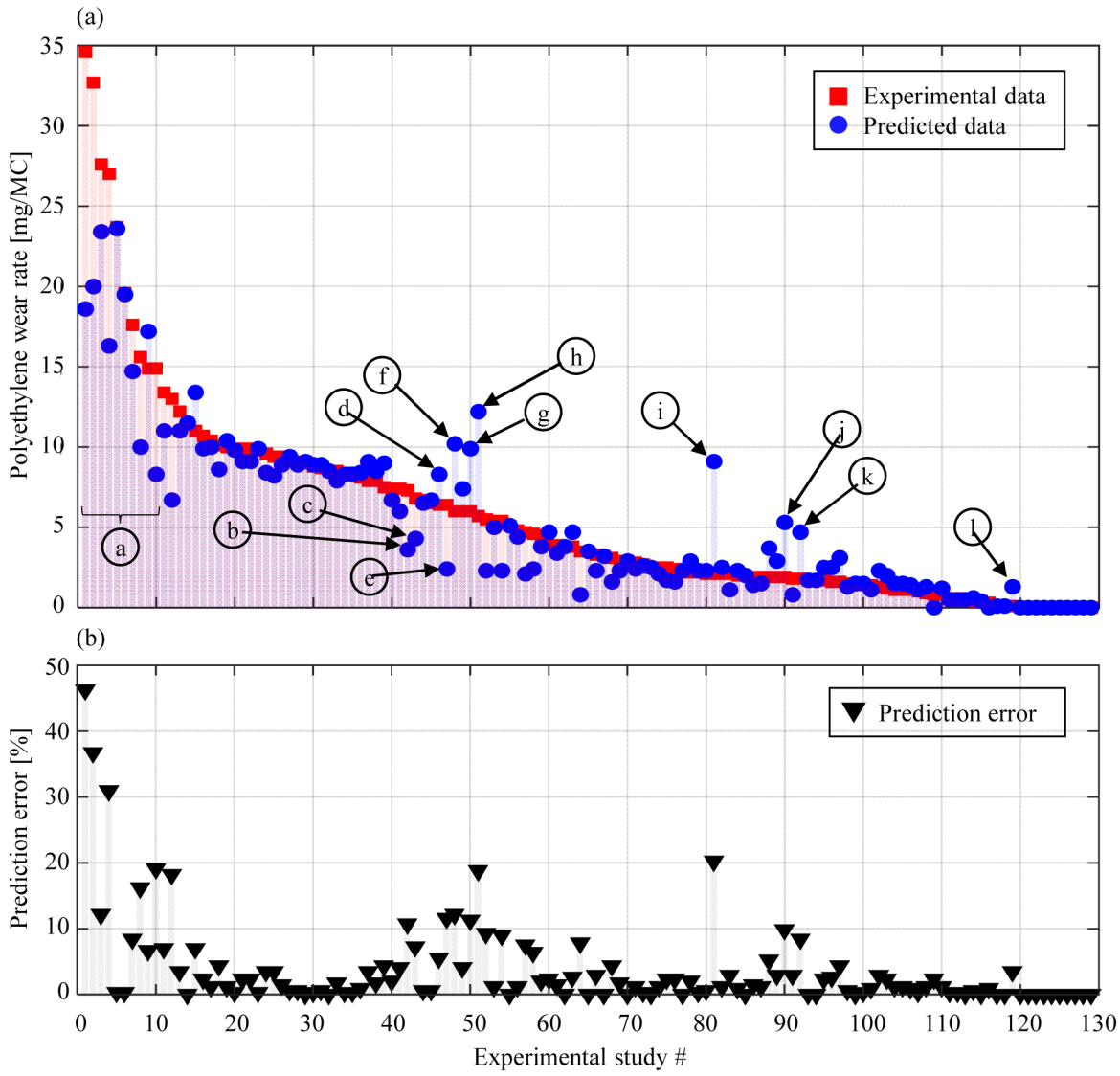

Figure 3.

Polyethylene wear rate for all experimental studies considered in our dataset ranked in descending order, (a) showing the experimental results documented in the literature (red square markers) and the corresponding predicted results using the data-driven model based on the KNN method (blue circle markers), and (b) showing the prediction error for the corresponding experimental study (black triangle markers)

Author Manuscript Author Manuscript Author Manuscript Author Manuscript

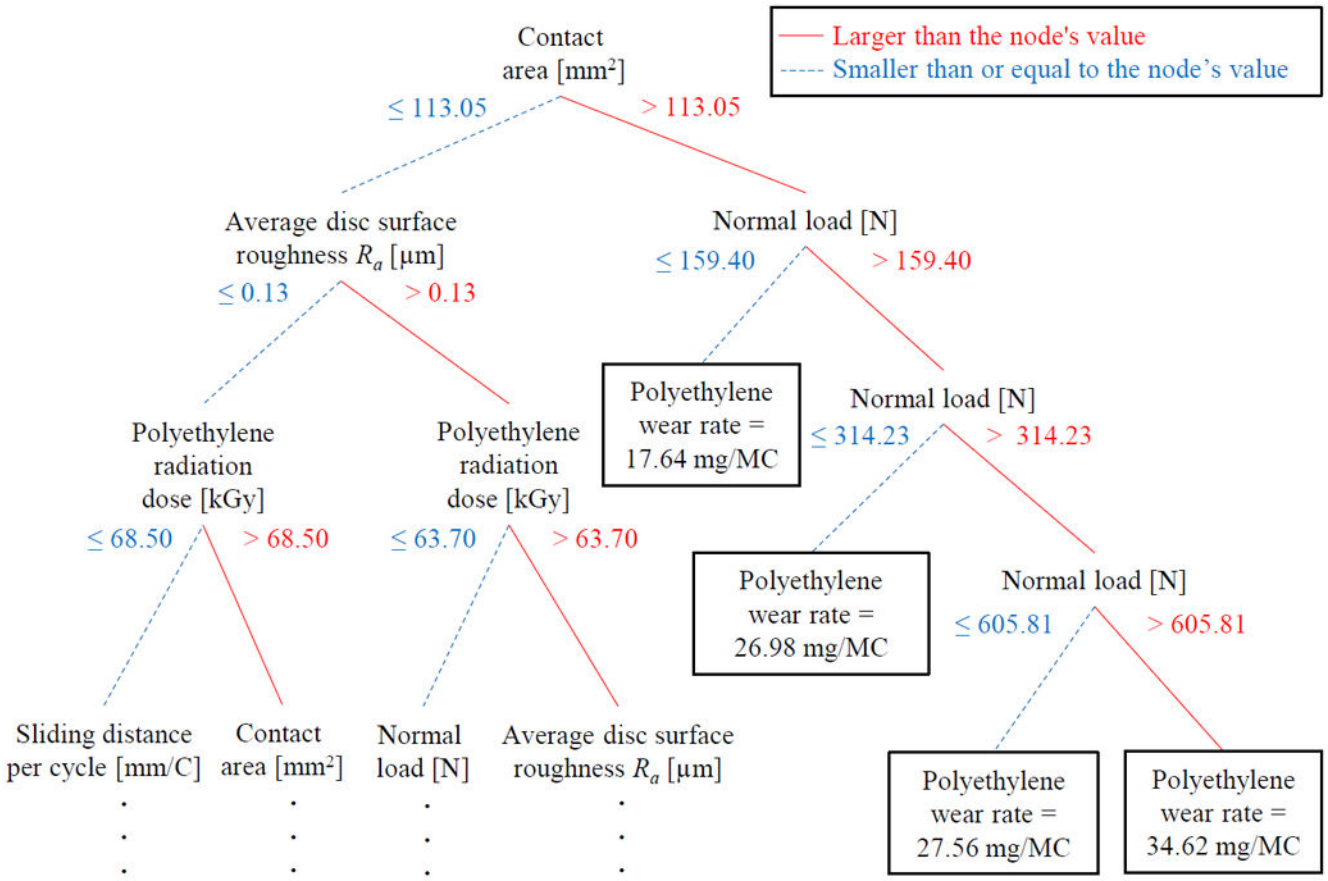

Figure 4.

First seven nodes of the CART model of the dataset considered in this work, showing how the attributes break down into a decision tree, ultimately predicting the target attribute and providing an interpretable model that relates the attributes (input) to the target attribute (output)

Author Manuscript

Author Manuscript

Author Manuscript

Author Manuscript

Table 1

Descriptive statistics of the polyethylene wear rate dataset, showing the same number of significant digits as in their respective publications

	Minimum	Maximum	Average	Standard deviation	Missing values	Stability [%]
Publication year	2001	2018	2008	6	0	20.16
Normal load [N]	7	777.55	166.26	129.38	0	28.68
Contact area [mm^2]	7.07	706.86	67.15	67.11	0	35.66
Frequency [Hz]	0.2	2	1.25	0.43	0	44.19
Sliding distance per cycle [mm/C]	17.76	94.25	30.47	10.08	0	30.23
Wear path shape	Rectangle 10 × 20 mm (used in 1 experiment)	Circle d=10 mm (used in 39 experiments)	-	-	0	30.23
Wear path aspect ratio	1	10.98	1.79	1.58	0	49.61
Lubricant temp. [°C]	20	37	29.23	7.50	63	46.97
Lubricant protein concentration [mg/ml]	0.69	64.8	22.28	6.35	33	36.46
Average disc surface roughness R_a [μm]	0.001	0.50	0.05	0.10	4	19.38
Polyethylene radiation dose [kGy]	0	150	36.31	40.77	0	40.31
Test duration [MC]	0.1	3.2	2.02	0.93	0	28.68
Polyethylene wear rate [mg/MC]	0.00	34.62	5.73	6.36	0	1.55

Author Manuscript

Author Manuscript

Author Manuscript

Author Manuscript

Table 2

Prediction error of each machine learning method used in this work, based on the entire polyethylene wear rate dataset

Method	***MAE***	***RMSE***	R^2
Model-based (interpretable)			
Linear Regression	3.44	4.72	0.71
CART	1.95	3.35	0.83
M5	3.13	4.82	0.78
Random Forest	2.87	4.04	0.75
Gradient boosting	2.69	4.03	0.72
Model-based (non-interpretable)			
ANN	3.33	4.86	0.73
SVM	3.20	4.45	0.69
Instance-based			
KNN	1.38	2.37	0.91

Author Manuscript

Author Manuscript

Author Manuscript

Author Manuscript

Table 3

Machine learning methods prediction error based on the polyethylene wear rate data for three subgroups

Polyethylene radiation dose [kGy]	**0 (Non-irradiated)**			**20-55 (Conventional)**			**>70 (HXPE)**		
Method	***MAE***	***RMSE***	***R^2***	***MAE***	***RMSE***	***R^2***	***MAE***	***RMSE***	***R^2***
Model-based (interpretable)									
Linear Regression	3.54	4.84	0.81	4.51	6.19	0.62	0.67	0.85	0.78
CART	2.67	3.43	0.77	2.39	3.62	0.81	0.70	0.99	0.77
M5	3.29	4.96	0.77	4.32	6.55	0.65	0.68	0.90	0.72
Random Forest	2.76	3.54	0.09	2.58	3.93	0.77	0.70	0.92	0.82
Gradient boosting	3.16	4.45	0.68	2.84	3.91	0.68	0.81	1.03	0.79
Model-based (non-interpretable)									
ANN	3.35	4.22	0.77	2.77	4.46	0.79	0.88	1.15	0.76
SVM	3.42	4.54	0.79	4.07	6.08	0.43	0.57	0.80	0.82
Instance-based									
KNN	2.16	3.08	0.87	1.24	1.97	0.81	0.50	0.75	0.88